Journal of Computational Physics 278 (2014) 485–496

Contents lists available at ScienceDirect

Journal of Computational Physics

www.elsevier.com/locate/jcp

Determining the effective resolution of advection schemes. Part I: Dispersion analysis

James Kent [a,*], Jared P. Whitehead [a,b], Christiane Jablonowski [a], Richard B. Rood [a]

[a] Department of Atmospheric, Oceanic and Space Science, University of Michigan, 2455 Hayward St., Ann Arbor, MI 48109-2143, USA
[b] Mathematics Department, Brigham Young University, 350 TMCB, Provo, UT, USA

ARTICLE INFO

Article history:
Received 28 August 2013
Received in revised form 15 January 2014
Accepted 26 January 2014
Available online 31 January 2014

Keywords:
Effective resolution
Finite-difference methods
Finite-volume methods
Dispersion relation analysis
Transport
Dynamical core

ABSTRACT

The effective resolution of a numerical scheme describes the smallest spatial scale (largest wavenumber) that is completely resolved by that scheme. Using dispersion relation analysis allows the effective resolution of a numerical scheme for the advection equation to be calculated. The advection equation is a fundamental building block of dynamical cores of atmospheric and ocean models, and this analysis provides an indication of the effective resolution of the numerical methods used by dynamical cores. Using a variety of finite-difference schemes, the effect on effective resolution of using explicit diffusion and hyper-diffusion terms is examined. The choice of order-of-accuracy, and the time-stepping of the numerical scheme is also investigated with regard to effective resolution. Finally, we apply this analysis to methods that are commonly used in dynamical cores of atmospheric general circulation models, namely semi-Lagrangian and finite-volume methods.

1. Introduction

Advection schemes are an important building block of atmospheric dynamical cores. The dynamical core is the fluid dynamics component of an atmospheric model, and it solves the adiabatic governing equations (usually the primitive equations under certain approximations, for example hydrostatic balance) and the equations governing the transport of tracers. As well as solving the transport equations, advection schemes can be modified to solve conservation laws, such as the continuity equation for fluid density, or the vorticity equation. There are many different types of numerical methods that are used for advection in dynamical cores of general circulation models (GCMs), such as finite-difference [8], finite-volume [20,38], semi-Lagrangian [4,47], and spectral element [5]. It is important to understand the properties of different numerical methods, either to better understand the properties of existing advection schemes and dynamical cores, or to make an informed modeling choice when designing future models.

One property of a numerical method is the effective resolution. Whereas 'resolution' usually refers to the model's grid spacing, the effective resolution of a numerical scheme is generally defined as the smallest spatial scale (i.e. the largest wavenumber) that is 'fully resolved' by said numerical scheme. The shortest fully resolved wavelength, i.e. the effective resolution, is usually considerably larger than the grid spacing [41]. It is desirable to determine the effective resolution of a numerical scheme, and therefore the effective resolution of a model that makes use of the scheme. For example, in atmospheric modeling there is a desire to resolve features that are unresolved or only marginally resolved by current models,

* Corresponding author. Tel.: +1 734 763 6241.
E-mail addresses: jdkent@umich.edu (J. Kent), whitehead@math.byu.edu (J.P. Whitehead), cjablono@umich.edu (C. Jablonowski), rbrood@umich.edu (R.B. Rood).

0021-9991/$ – see front matter
http://dx.doi.org/10.1016/j.jcp.2014.01.043

and thus improve weather forecasts and climate predictions [31]. As a higher effective resolution means that more features will be resolved by the model, increasing a model's effective resolution (through the choice of numerical methods) could prove a cheaper alternative than just doubling the grid resolution. This idea is closely related to the concept of 'equivalent resolution' as discussed in [46].

In addition, understanding the effects of explicit diffusion and filters on effective resolution provides insight into the tuning of diffusion coefficients (and the consequences of badly tuned parameters). With full GCMs the coupling of the subgrid-scale physical parameterization package and the "resolved" dynamical core is an important issue [6], and the physics parameterizations are often coupled to the dynamics at the grid scale. However, the dynamics do not truly resolve the grid scale, and it may be beneficial to add some of the physics to only the resolved scales i.e. the effective resolution [16]. Such GCM experiments with finer grid spacings in the dynamical core and coarser grids for the physics forcings were evaluated by Williamson [44]. For weather and climate models, composed of both dynamics and physics, Skamarock [31] suggested numerically calculating the effective resolution based upon the departure of the kinetic energy spectra from a given power law. However, analytical methods can be used to calculate the effective resolution of linear advection schemes, as proposed in this paper.

One tool to evaluate the properties of numerical schemes is dispersion relation analysis [28]. Linear dispersion relation analysis and von Neumann stability analysis of numerical schemes for atmospheric models has previously been performed for a variety of methods and equation sets [22,25,17,32]. This analysis can be used to investigate dispersive properties (such as group velocity and phase speed) and diffusive properties, and can be used to determine accuracy and stability of the numerical scheme [36,42]. Using this analysis to measure the effective resolution of a numerical method was introduced by Ullrich [40]. In [40], several different types of numerical methods (finite-volume, spectral element, spectral finite-volume, and discontinuous Galerkin) were analyzed for the linear wave equation with exact time integration, and their dispersive and diffusive properties were used to determine the effective resolution for different orders of accuracy. The aim of our paper is to modify this analysis for use with different time integration methods, to show the impact of the time integration scheme and the choice of timestep on the effective resolution of advection schemes. We also investigate the effect of explicit diffusion and hyper-diffusion terms on the diffusive and dispersive properties of a numerical scheme, and therefore the impact this diffusion has on effective resolution. We investigate these issues using simple finite-difference schemes, before applying the analysis to methods that are commonly used in transport schemes for dynamical cores; semi-Lagrangian and finite-volume methods. The assessment of the effective resolution of schemes for the advection equation is a first step towards investigating the effective resolution of the non-linear dynamics component of a GCM. There are many different types of advection schemes (see, for example, [30]). Our paper is not meant to be a comprehensive study of all advection schemes, but introduces the concept of calculating the effective resolution through a variety of possible choices in the algorithm. Although our focus is on numerical methods for atmospheric dynamical cores, the analysis can be applied to advection schemes that are used in any field of numerical analysis.

Some form of diffusion (either implicit in the numerics, as an explicitly added term, or in the form of a filter) is usually required for models solving non-linear governing equations on a fixed grid. In numerical studies of three-dimensional turbulence (large eddy simulation – LES) a subgrid model is required to dissipate kinetic energy, as this represents the effects of the unresolved flow on the resolved flow [23]. For two-dimensional flow it is the enstrophy which cascades downscale to unresolved scales, and therefore must be dissipated [13]. The atmosphere is strongly multiscale, with many interactions between these scales. Due to the effects of stratification and rotation, the atmosphere may resemble two-dimensional flow at large scales [1], before transitioning to three-dimensional flow at smaller scales. In dynamical cores of atmospheric models the diffusion is used to prevent the accumulation of potential enstrophy and kinetic energy at the grid scale, and also to dissipate tracer variance in the transport scheme [33,14]. This diffusion is often added in an ad-hoc way, and heavily tuned to provide optimal results [12]. For the constant velocity linear advection equation there are no diffusion effects in the true solution, although there are a number of numerical reasons that a modeler might chose to add diffusion to their scheme (for example to improve stability, to damp computational modes, or to ensure monotonicity). This means that although diffusion is undesired in the linear dispersion analysis for the linear advection equation, it is an essential part of the numerical methods that make up the dynamical cores. For this reason we consider the effects of some of the different forms of diffusion on the effective resolution of advection schemes.

This paper is structured as follows. Section 2 describes the one-dimensional linear advection equation and the dispersion relation and von Neumann analysis methodology. Using the dispersion relation analysis to determine the effective resolution of a number of numerical schemes is presented in Section 3, where we use finite-difference schemes to show the effects of order-of-accuracy, diffusion and time-stepping on effective resolution. We then turn our attention to numerical methods that are commonly used in dynamical cores, such as semi-Lagrangian and finite-volume methods. Conclusions are drawn in Section 4.

2. The advection equation

The one-dimensional advection equation is given as

$$\frac{\partial q}{\partial t} + u\frac{\partial q}{\partial x} = 0, \tag{1}$$

where $q(x,t)$ is a tracer mixing ratio, u is the constant velocity, x is the horizontal direction and t is time. Note that all quantities are dimensionless in this paper, and that throughout we use $u = 1$. Since u is constant, the one-dimensional linear advection equation can also be written in flux form as

$$\frac{\partial q}{\partial t} + \frac{\partial uq}{\partial x} = 0. \tag{2}$$

Note that for non-constant velocities the flux form must be written in terms of a tracer density, and that the form given here is for the special case of constant density. The advective form (1) and the flux form (2) are interchangeable for constant velocities. The advection equation supports wavelike solutions of the form

$$q = \hat{q}\exp\big(i(kx - \omega t)\big), \tag{3}$$

where k is the spatial wavenumber, ω the frequency, $\hat{q}$ is the amplitude, and $i = \sqrt{-1}$ is the imaginary unit. The wavelike solutions allow the calculation of the dispersion relation (which can also be used to calculate the phase speed and the group velocity) as

$$\omega = \omega(k) = uk, \tag{4}$$

and the amplitude factor

$$|\Gamma| = \big|\exp(-i\omega t)\big| = 1. \tag{5}$$

For numerical solutions to the advection equation an important quantity is the Courant number $c = u\Delta t/\Delta x$, where Δt is the timestep and Δx is the grid spacing. The Courant number is linked to the stability of a numerical scheme (it is common for methods to be unstable for $c > 1$). In fluid dynamics problems the velocity u is rarely constant, and therefore in this paper we consider the analysis over a number of Courant numbers. In this paper we only consider the case of uniform grid spacing, i.e. constant Δx.

To calculate the amplitude factor and dispersion relation of a given numerical scheme we use von Neumann analysis and insert the solution for the discrete tracer

$$q_j^n = \hat{q}\exp\big(i(kx_j - \omega t_n)\big), \tag{6}$$

into the scheme's discretization. Here j and n are the spatial and temporal indices, with $\Delta x = x_{j+1} - x_j$ and $\Delta t = t_{n+1} - t_n$. We divide each term in the discretization by (6), to give a relationship between the numerical amplitude factor $|\Gamma| = |\exp(-i\omega\Delta t)|$ and k. The amplitude factor $|\Gamma|$ shows which wavenumbers k are damped or amplified by the numerical scheme. If the amplitude factor exceeds 1 for any k, then the scheme is unstable.

For a two-time-level scheme, the resulting expression for the scheme's discretization will only contain the amplitude factor to the power one. For a three time-level scheme we obtain an expression which is quadratic in Γ, and thus requires the solution to the quadratic equation to give the amplitude factor in terms of k. Similarly, a four time-level scheme gives a cubic equation. Note that the correct root must be selected to give the actual amplitude factor of the physical mode, and not that of the computational modes.

We proceed by first calculating the amplitude factor and then the dispersion relation. Comparing a numerical scheme's dispersion relation with the true dispersion relation shows which wavenumbers are properly capturing the dispersive properties of the advection equation. The numerical dispersion relation can be computed via (5) as

$$\omega = -\frac{\log\Gamma}{i\Delta t}. \tag{7}$$

We are interested in comparing the effect of choosing various timesteps for a given spatial grid. In order to provide a fair comparison, we evaluate the cumulative effect of the schemes over the distance Δx. This is equivalent to saying that for a Courant number of $c = 0.1$ the analysis must be repeated 10 times to give the corresponding result for analysis performed with $c = 1$. To make the analysis consistent, unless noted otherwise, we run to $c = 1$. This means that we evaluate the numerical schemes as they transport q over the distance Δx. Therefore, we set the number of timesteps as $m = 1/c$ and calculate the numerical amplitude factor as

$$|\Gamma_N| = \big|\Gamma^m\big|, \tag{8}$$

and the numerical dispersion relation as

$$\omega_N = -\frac{\log\Gamma^m}{i\Delta t m}. \tag{9}$$

3. Determining effective resolution

Following [10,40] we define a wavenumber k as being 'fully resolved' by a numerical scheme if the numerical scheme satisfies both the dispersive and diffusive properties of the advection equation at that wavenumber. The numerical dispersion relation ω_N is classed as satisfied at wavenumber k if

$$\frac{|Re(\omega) - Re(\omega_N)|}{|Re(\omega)|} \leqslant \epsilon, \tag{10}$$

for wavenumber k at some error threshold ϵ. Similarly, the diffusive property is satisfied using the numerical amplitude factor Γ_N at wavenumber k if

$$\frac{||\Gamma| - |\Gamma_N||}{|\Gamma|} \leqslant \epsilon, \tag{11}$$

for wavenumber k. The true dispersion relation and amplitude factor are given by (4) and (5). The effective resolution of a numerical scheme is thus defined as the shortest wave (with wavelength $N\Delta x$) which satisfies both the dispersion relation (10) and the diffusive property (11) metrics, for all waves with wavelength $\lambda \geqslant N\Delta x$. Therefore, a scheme has a better effective resolution and can resolve smaller scales for smaller values of N. Note again that in these calculations we take the cumulative amplitude factors and dispersion relations, (8) and (9), as we perform the analysis on the numerical scheme as it transports q over the distance of one grid space, Δx (i.e. using $m = 1/c$ in (8) and (9)).

The choice of the threshold ϵ has a large impact on which wavenumbers are classified as resolved. Following [40] we choose $\epsilon = 0.01$, i.e. the numerical dispersion relation and amplitude factor must be within 99% of the analytic value. This threshold corresponds to a wave being damped by 10% over approximately $10\Delta x$, and being completely out of phase over the distance $\pi\Delta x/0.01$. Note that we are weighting the diffusive and dispersive errors equally, and that it would be viable to use different ϵ for diffusion and dispersion errors when calculating the effective resolution.

We use this methodology to investigate the effective resolution of advection schemes. We use simple finite-difference schemes as a general case to highlight the effects of three modeling choices: order of accuracy; explicit diffusion; and time-stepping. We then focus on numerical methods that are relevant to tracer transport and dynamical cores, investigating semi-Lagrangian schemes (Section 3.4) and finite-volume schemes (Section 3.5).

3.1. Order of accuracy

In general, for smooth data, a numerical method with a higher formal order of accuracy will be more accurate than a scheme with a lower order of accuracy. However, increasing the order of accuracy of a numerical scheme is usually computationally expensive, especially for multi-dimensional schemes. Hence there is a need to consider the effect of increased accuracy with increased cost [15]. In this section we show the effects of increased accuracy on effective resolution.

ADER (Arbitrary-order DErivative Riemann) schemes are finite-volume methods used to solve conservation laws using monotonic limiters [34,27], although they can easily be written as finite-difference schemes for the linear advection equation. They have the same temporal and spatial orders of accuracy, and hence they can be used to investigate the effect of the order of accuracy of a numerical scheme on the effective resolution. Note that for our analysis we use ADER schemes without any limiters. The use of limiters makes these schemes non-linear, whereas the dispersion relation analysis and von Neumann stability analysis can only be applied to linear schemes. The linear advection equation is solved as

$$q_j^{n+1} = q_j^n - c\left(\tilde{q}_{j+\frac{1}{2}}^{n+\frac{1}{2}} - \tilde{q}_{j-\frac{1}{2}}^{n+\frac{1}{2}}\right), \tag{12}$$

with the flux-like terms $\tilde{q}_{j-\frac{1}{2}}^{n+\frac{1}{2}}$ calculated to the desired order of accuracy. Here the half spatial indices relate to the midpoint between finite-difference points (or the cell edges of finite-volume cells). The well known Lax–Wendroff scheme [19], which calculates the flux-like terms as

$$\tilde{q}_{j-\frac{1}{2}}^{n+\frac{1}{2}} = \frac{1}{2}\left(q_j^n + q_{j-1}^n\right) - \frac{1}{2}c\left(q_j^n - q_{j-1}^n\right), \tag{13}$$

can be classed as a second-order ADER scheme. It is evident that the Lax–Wendroff/ADER schemes can be written in flux form (2), with the numerical fluxes given by $u\tilde{q}_{j\pm\frac{1}{2}}^{n+\frac{1}{2}}$. As the Lax–Wendroff/ADER schemes can be extended up to arbitrary order of accuracy [35], we use orders 2–6, and also include the first-order upwind scheme in our analysis.

Fig. 1 shows the maximum resolved wave (in terms of $N\Delta x$) for $\epsilon = 0.01$ for the Lax–Wendroff/ADER schemes for Courant numbers $0 < c \leqslant 1$. The effective resolution when only the diffusive component is considered is shown in the left plot. The effective resolution when only the dispersive component is considered is shown in the center plot. The right plot shows the effective resolution when both the diffusive and dispersive components are considered, and therefore is the maximum of the left and center plot for each Courant number. Note that the first-order and fifth-order schemes have zero

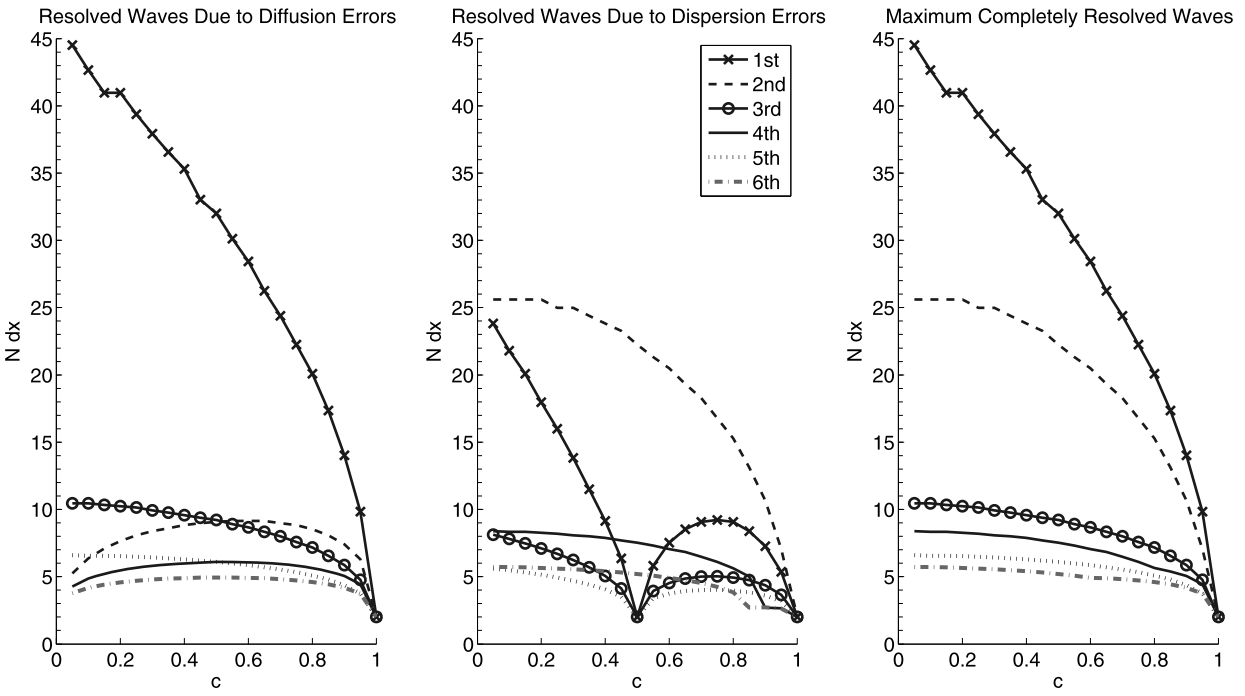

Fig. 1. The maximum resolved wave (in terms of $N\Delta x$) for $\epsilon = 0.01$ due to diffusion errors (left), dispersion errors (center), and both diffusion and dispersion error (right), for Lax–Wendroff/ADER schemes of order 1 to 6. The right plot is therefore the maximum of the left and center plots. The smallest possible resolved wave is $N = 2\Delta x$.

dispersion errors at $c = 0.5$. At $c = 1$, for each order scheme both the diffusive and dispersive error terms become zero, meaning that the schemes have zero error for $c = 1$. Hence the effective resolution reverts to $2\Delta x$ at $c = 1$.

As seen in the right plot of Fig. 1, the increase in order of accuracy results in a higher effective resolution, as expected. However, the level of improvement decreases as the order of accuracy gets higher. For example, the increase in effective resolution from first- to second-order is approximately $20\Delta x$ for $c = 0.05$, and the increase from fourth- to fifth-order is approximately $2\Delta x$ for $c = 0.05$.

These results can also show us the effectiveness of increasing the grid resolution. For example, for $c = 0.05$ the second-order Lax–Wendroff scheme has an effective resolution of approximately $26\Delta x$. Doubling the grid resolution would result in the second-order Lax–Wendroff scheme resolving $26\Delta x$ of the fine grid, and $13\Delta x$ of the original, coarse grid. However, the third-order ADER scheme resolves approximately $10\Delta x$ on the original, coarse grid. This implies that it is beneficial (in terms of number of resolved waves) to use the third-order ADER scheme on the coarse grid rather than the second-order Lax–Wendroff scheme on the finer grid.

3.2. Effect of explicit diffusion

Explicit diffusion terms can be applied to any scheme for the advection equation. Here we use the second-order Lax–Wendroff scheme used in the previous section for simplicity. The coefficients in this section are chosen to illustrate the effects of diffusion on effective resolution. When additional hyper-diffusion terms of order $2p$ are used, the advection equation becomes the advection–diffusion equation of the form

$$\frac{\partial q}{\partial t} + u\frac{\partial q}{\partial x} = (-1)^{p+1}\mu_p \frac{\partial^{2p} q}{\partial x^{2p}}, \tag{14}$$

for $p = 1, 2, 3, 4, \ldots$, where μ_p is the diffusion coefficient. The diffusion coefficient is chosen as $\mu_p = \nu_p \Delta x^{2p}/\Delta t$, where ν_p is a constant. For the analysis in this paper we approximate second-order diffusion as

$$\frac{\partial^2 q}{\partial x^2} \approx \frac{1}{\Delta x^2}\left(q^n_{j+1} - 2q^n_j + q^n_{j-1}\right). \tag{15}$$

The use of second-order diffusion with the second-order Lax–Wendroff scheme is shown in Fig. 2. Three diffusion coefficients are used, each increasing in magnitude by a factor of two. The use of explicit diffusion increases the diffusion errors of the scheme, but it can also remedy some of the dispersion errors in the second-order Lax–Wendroff scheme. The choice of diffusion coefficient becomes important, as it is desirable to decrease dispersion errors without producing too many diffusion errors. Using explicit diffusion and the 'right' coefficient with the second-order Lax–Wendroff scheme can improve

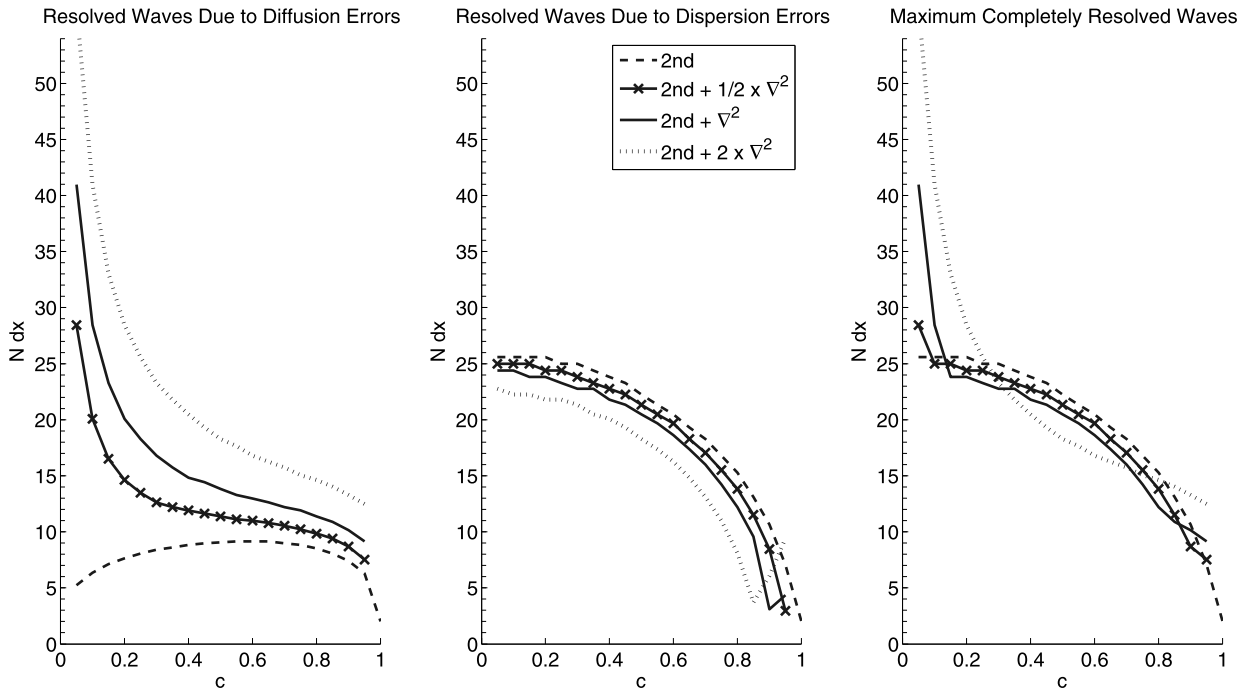

Fig. 2. The maximum resolved wave (in terms of $N\Delta x$) for $\epsilon = 0.01$ due to diffusion errors (left), dispersion errors (center), and both diffusion and dispersion error (right), for the second-order Lax–Wendroff scheme with ∇^2 diffusion of different coefficient strength.

the effective resolution of the scheme. In general, adding the diffusion terms reduces the dispersion error, and therefore the schemes with the diffusion and hyper-diffusion achieve (nearly) zero dispersive error at Courant numbers less than 1 (as opposed to $c = 1$ for the Lax–Wendroff/ADER schemes). Then as $c \to 1$, the additional diffusion terms do not cancel the dispersion errors, and the resolved waves due to dispersion errors increase for each of the schemes with diffusion.

We also consider the effects of higher-order hyper-diffusion applied to the fourth-order ADER scheme. The results (not shown) agree with the second-order diffusion, in that the hyper-diffusion increases diffusion errors, but decreases dispersion errors. The lower ordered hyper-diffusion, e.g. fourth- and sixth-order, has the most effect on the diffusion and dispersion errors, with higher-order hyper-diffusion (eighth-order and above, i.e. $p \geqslant 4$ in (14)) having almost no impact on the effective resolution of the fourth-order scheme.

3.3. Time-stepping scheme

Section 3.1 shows the effective resolution when forward-in-time, Lax–Wendroff/ADER time-stepping is used. However, as the Lax–Wendroff scheme is rarely used in current transport schemes or dynamical cores we investigate more commonly used time-stepping methods. Here we show the effective resolution for second- and fourth-order spatial schemes with different types of time-stepping. In this paper, the spatial derivative is approximated using the second-order approximation

$$\frac{\partial q_j^n}{\partial x} \approx \frac{1}{2\Delta x}\left(q_{j+1}^n - q_{j-1}^n\right), \tag{16}$$

and the fourth-order approximation

$$\frac{\partial q_j^n}{\partial x} \approx \frac{1}{12\Delta x}\left(-q_{j+2}^n + 8q_{j+1}^n - 8q_{j-1}^n + q_{j-2}^n\right). \tag{17}$$

We consider leapfrog, Adams–Bashforth [7], Runge–Kutta [9], and implicit time-centered time-stepping schemes.

The leapfrog scheme is temporally second-order, and discretizes the advection equation as a centered difference approximation in time

$$q_j^{n+1} = q_j^{n-1} - 2u\Delta t\frac{\partial q_j^n}{\partial x}. \tag{18}$$

Leapfrog time-stepping is common with both spectral and finite difference methods (such as the vertical discretization of [8]). The third-order Adams–Bashforth method [7] makes use of data at four-time levels, and is discretized as

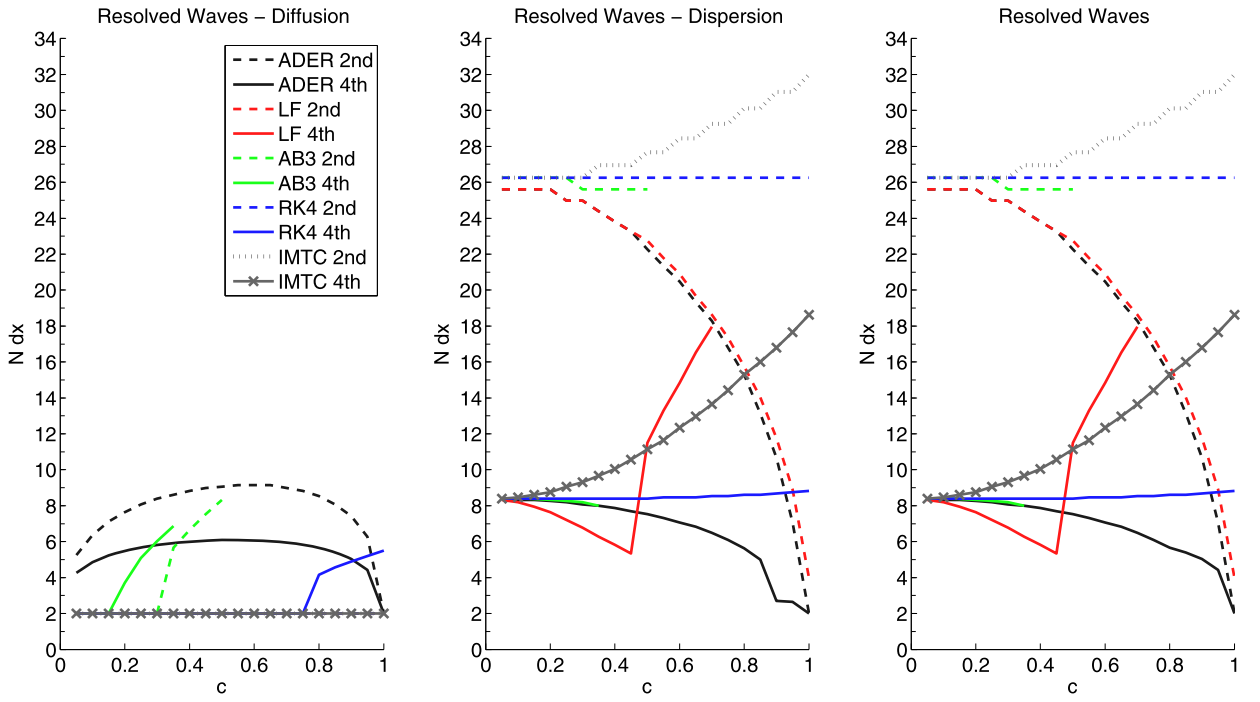

Fig. 3. The maximum resolved wave (in terms of $N\Delta x$) for $\epsilon = 0.01$ due to diffusion errors (left), dispersion errors (center), and both diffusion and dispersion error (right), for leapfrog (LF), third-order Adams–Bashforth (AB3), fourth-order Runge–Kutta (RK4) and implicit time-centered (IMTC) schemes with spatial order 2 and 4. Also shown are the second and fourth-order Lax–Wendroff/ADER schemes (ADER) from Fig. 1. The right plot is the maximum of the left and center plots, and as the dispersion errors dominate for each of these schemes, the right plot and center plot are identical (apart from the fourth-order ADER scheme). The lines that end before $c = 1$ show the stability limit of the schemes, i.e. the last stable Courant number for that scheme.

$$q_j^{n+1} = q_j^n - u\frac{\Delta t}{12}\left(23\frac{\partial q_j^n}{\partial x} - 16\frac{\partial q_j^{n-1}}{\partial x} + 5\frac{\partial q_j^{n-2}}{\partial x}\right). \tag{19}$$

The Runge–Kutta schemes are a family of time-stepping schemes that have been used in a variety of atmospheric problems [11,37,43]. Here we use the fourth-order version [9], given as

$$k_1 = \frac{\partial q_j^n}{\partial x}, \qquad k_2 = \frac{\partial (q_j^n - 0.5u\Delta t k_1)}{\partial x}, \tag{20}$$

$$k_3 = \frac{\partial (q_j^n - 0.5u\Delta t k_2)}{\partial x}, \qquad k_4 = \frac{\partial (q_j^n - u\Delta t k_3)}{\partial x}, \tag{21}$$

$$q_j^{n+1} = q_j^n - u\frac{\Delta t}{6}(k_1 + 2k_2 + 2k_3 + k_4). \tag{22}$$

Implicit time-stepping schemes are used because they are generally unconditionally stable, although they require the solution of an elliptic equation at each timestep. The implicit time-centered scheme, which is temporally second-order, is discretized as

$$q_j^{n+1} = q_j^n - u\frac{\Delta t}{2}\left(\frac{\partial q_j^{n+1}}{\partial x} + \frac{\partial q_j^n}{\partial x}\right). \tag{23}$$

Fig. 3 shows the effective resolution for second and fourth-order spatial schemes when using leapfrog, Adams–Bashforth, Runge–Kutta and implicit time-centered time-stepping. The plots end at the Courant number that the schemes become unstable, and this shows the stability limits of the fourth-order leapfrog scheme and of the Adams–Bashforth schemes for advection. For comparison, the second- and fourth-order Lax–Wendroff/ADER schemes are also shown. As we use second and fourth-order spatial order of accuracy the diffusion errors are small and the dispersion errors dominate. Therefore the effective resolution is almost completely decided by the dispersive errors, and the center and right plots of Fig. 3 are almost identical. The plot shows how the spatial order dominates the effective resolution, with the second-order spatial schemes resolving around $25\Delta x$ and the fourth-order spatial schemes resolving around $8\Delta x$ (for small Courant numbers). The plot also shows the sensitivity to the time-stepping method. Similar to the Lax–Wendroff schemes, the effective resolution of the second-order leapfrog scheme improves as the Courant number approaches unity. The Runge–Kutta time-stepping produces similar results to the Adams–Bashforth method, except that the Runge–Kutta methods are stable for all shown Courant

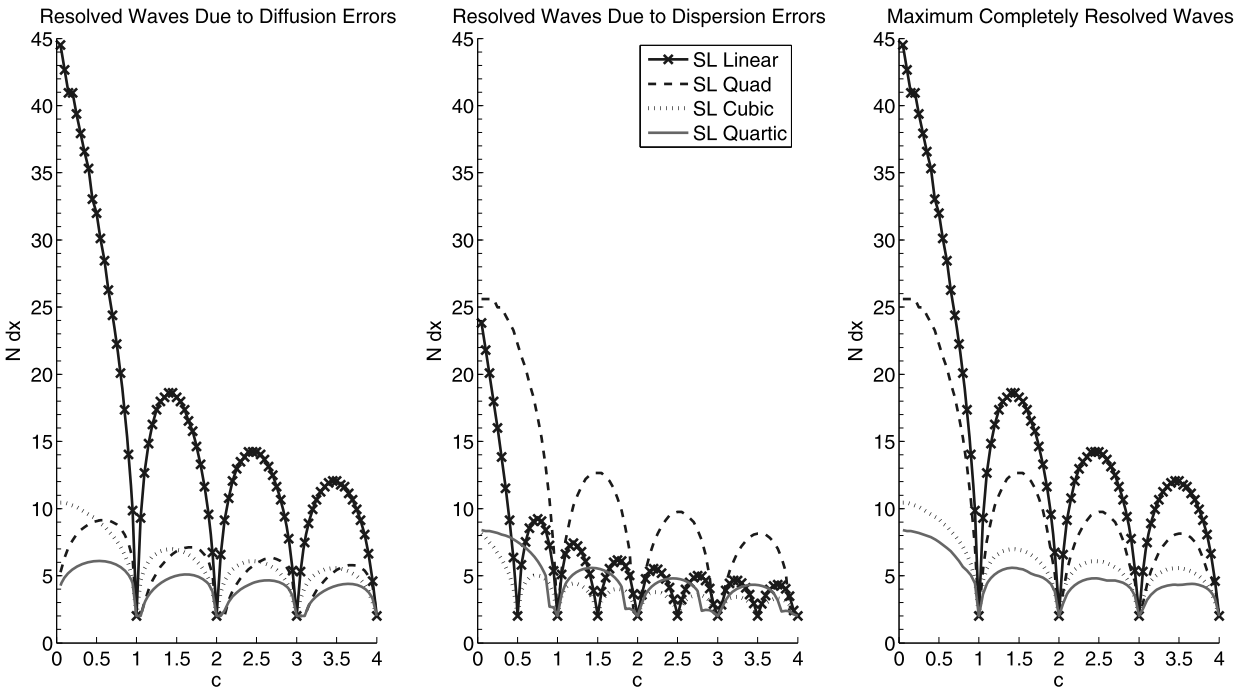

Fig. 4. The maximum resolved wave (in terms of $N\Delta x$) for $\epsilon = 0.01$ due to diffusion errors (left), dispersion errors (center), and both diffusion and dispersion error (right), for two-time-level semi-Lagrangian (SL) schemes with linear, quadratic, cubic and quartic interpolation.

numbers. As the Runge–Kutta method is temporally fourth-order, for the fourth-order spatial schemes there is not the sudden increase in the dispersion errors around $c \approx 0.4$ that can be seen for the spatially fourth-order and temporally second-order leapfrog scheme. For the implicit time-centered method the effective resolution gets worse as the Courant number increases. This is due to the accuracy of the time-stepping (second-order for implicit time-centered) degrading with increased timestep Δt.

The Robert–Asselin time filter [29,2] is a method to damp the computational mode associated with the leapfrog scheme. It is commonly used for models that employ a three-time-level approach such as the Community Atmosphere Model Eulerian (CAM-EUL) spectral transform dynamical core [26]. It is an approximation of the second temporal derivative, and is discretized as

$$q_j^n = \kappa q_j^{n+1} - (2\kappa - 1) q_j^n + \kappa q_j^{n-1}, \tag{24}$$

where κ is the filter coefficient. Considering different strength filter coefficients (not shown), the effect of the time-filter is similar to the explicitly added spatial diffusion as seen in Fig. 2: the time filter can reduce the dispersion errors and can produce a higher effective resolution than if no filter is used, although a large filter coefficient results in very large diffusion errors.

3.4. Semi-Lagrangian schemes

Semi-Lagrangian schemes were historically used in dynamical cores that made use of latitude–longitude grids [45]. This was to reduce the impact of the convergence of the meridians at the pole, and allow larger timesteps to be taken. Semi-Lagrangian schemes are often used for transport in global spectral models, as it is easier to ensure positivity with semi-Lagrangian schemes than with spectral methods. Recent advances, such as conservative and high-order monotonic versions [18,48,39], indicate that semi-Lagrangian methods still have a part to play in the next generation of dynamical cores.

Here we use semi-Lagrangian schemes with no limiting. The semi-Lagrangian schemes can be written in finite-difference formulation, as given by [24]. For example, the semi-Lagrangian scheme with linear interpolation is given as

$$q_j^{n+1} = \alpha q^n_{j-(1+\mathrm{int}(c))} + (1-\alpha) q^n_{j-\mathrm{int}(c)}, \tag{25}$$

where $\alpha = c - \mathrm{int}(c)$. The formula for quadratic, cubic and quartic interpolation is given by [24].

The effective resolution of semi-Lagrangian schemes using linear, quadratic, cubic and quartic interpolation is shown in Fig. 4. One of the strengths of the semi-Lagrangian scheme is that it remains stable for long timesteps with $c > 1$. For this

reason we show results up to Courant number $c = 4$, although to be consistent with the other schemes in this paper we assume that they are only simulated until $c = 1$, i.e. $m = 1/c$ in (8). The results for $c \leqslant 1$ are identical to those obtained using the Lax–Wendroff/ADER schemes of order one to four, shown in Fig. 1. For integer Courant numbers the advection is exact, and therefore all schemes are able to resolve the $2\Delta x$ wave. For each scheme, the pattern of diffusion and dispersion errors follows a similar quadratic curve between integer Courant numbers. The magnitude of this pattern decreases as the Courant number increases, because the simulation is only run to time $c = 1$.

The results for the semi-Lagrangian scheme with $c > 1$ are identical to those that can be obtained by running the Lax–Wendroff/ADER schemes (of order one to four) with a long time-step extension, such as the flux-form semi-Lagrangian approach of [21]. Note that these schemes are only equivalent for the linear constant velocity advection Eq. (1) that is considered in our paper.

3.5. Finite-volume schemes

Finite-volume methods contain a number of desirable qualities (such as conservation, ease of applying limiters, and being a local method) and as such have been used in a number of transport schemes and dynamical cores of GCMs (for example [20,38]).

The flux form Eq. (2) is numerically solved using fluxes F as

$$\frac{\partial q_j}{\partial t} = -\frac{\left(F^{n+\frac{1}{2}}_{j+\frac{1}{2}} - F^{n+\frac{1}{2}}_{j-\frac{1}{2}}\right)}{\Delta x}, \tag{26}$$

where the fluxes are calculated using subgrid distributions, $\tilde{q}$. The subgrid distributions make use of the cell volumes and cell edge reconstructions, $q_{j\pm\frac{1}{2}}$, and the type of distribution determines which finite-volume scheme is being used. For distributions that are discontinuous at the cell edges a Riemann flux operator is used. For the linear advection equation (with positive u) this becomes the upwind flux

$$F_{j+\frac{1}{2}} = u\tilde{q}_j\left(x_j + \frac{\Delta x}{2}\right), \tag{27}$$

and for continuous distributions the flux is given as

$$F_{j+\frac{1}{2}} = uq_{j+\frac{1}{2}}. \tag{28}$$

Finite-volume methods have much in common with conservative finite-difference schemes (for example, the ADER schemes calculate fluxes and can easily be applied to the conservative form or the advective form of the equation), and as such, for the linear advection equation some finite-volume methods are equivalent to some of the finite-difference schemes discussed in this paper. For example, the finite-volume method with piecewise constant subgrid distribution is just the first-order upwind scheme. The fourth-order centered edge reconstruction

$$q_{j+\frac{1}{2}} = \frac{-q_{j+2} + 7q_{j+1} + 7q_j - q_{j-1}}{12} + O\left(\Delta x^4\right) \tag{29}$$

becomes the fourth-order approximation of $\partial q/\partial x$ given by (17).

To investigate the effective resolution of finite-volume methods we use the second-order and third-order upwind schemes from [36], with fourth-order Runge–Kutta time-stepping. We also use the unlimited piecewise parabolic method (PPM) of [3]. PPM uses the fourth-order edge reconstruction (29) to calculate $q_{j+\frac{1}{2}}$ and a parabolic subgrid distribution that makes the overall scheme third-order accurate. We also show results for both the second and third-order edge reconstructions (again with the parabolic subgrid distribution). Normally a limiting procedure is applied to make the reconstruction piecewise and discontinuous at cell edges, so that in each cell $qR_j = \tilde{q}_j(x_j + \frac{\Delta x}{2})$ and $qL_j = \tilde{q}_j(x_j - \frac{\Delta x}{2})$. Here, qL_j and qR_j are the left and right edge reconstructions of cell j. In the linear analysis applied in this paper no limiting is used, so that $qR_j = qL_{j+1} = q_{j+\frac{1}{2}}$. The flux is then calculated as

$$F_{j+\frac{1}{2}} = qR_j - \frac{c}{2}\left(qR_j - qL_j - \left[1 - \frac{2c}{3}\right](6q_j - 3qL_j - 3qR_j)\right). \tag{30}$$

Fig. 5 shows the effective resolution of the above mentioned finite-volume schemes for Courant numbers between 0 and 1. As with the finite-difference methods, the second-order scheme's effective resolution is dominated by dispersion errors, whereas the third-order scheme's effective resolution is dominated by diffusion errors, and the third-order upwind scheme can resolve smaller scales than the second-order upwind scheme. The Runge–Kutta time-stepping for the finite-volume schemes produces similar results to the Runge–Kutta time-stepping with finite-difference schemes (Fig. 3). For PPM, increasing the order of accuracy of the edge reconstruction improves the effective resolution, similar to increasing the order of accuracy of the Lax–Wendroff/ADER schemes. PPM with the third-order edge reconstruction becomes unstable for $c > 0.6$. PPM with the fourth-order edge reconstruction outperforms, in terms of effective resolution, all the other finite-volume methods tested here, for all $0 < c \leqslant 1$.

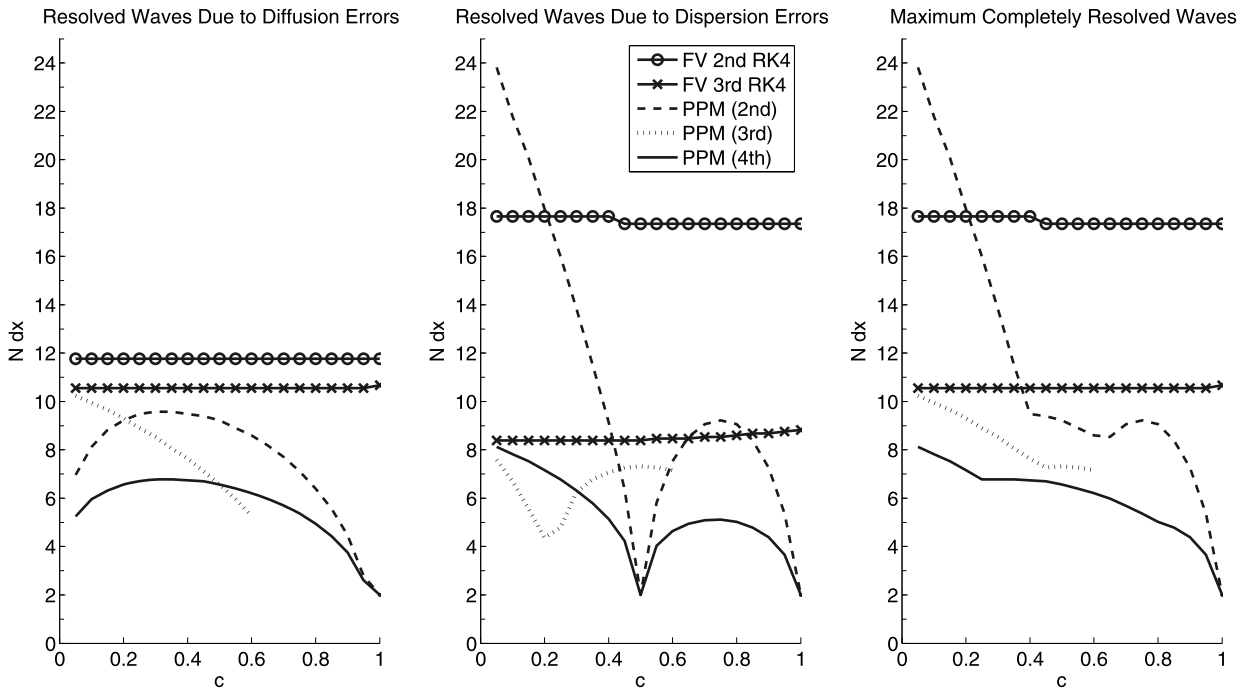

Fig. 5. The maximum resolved wave (in terms of $N\Delta x$) for $\epsilon = 0.01$ due to diffusion errors (left), dispersion errors (center), and both diffusion and dispersion error (right), for the second-order upwind with Runge–Kutta 4 time-stepping, the third-order upwind with Runge–Kutta 4 time-stepping, and the piecewise parabolic method (PPM) with second, third and fourth-order edge reconstructions, finite-volume schemes.

4. Discussion and conclusions

The effective resolution of a numerical scheme is the smallest scale that is fully resolved by that numerical scheme. We have provided a method to analytically determine the effective resolution of numerical schemes for the linear advection equation using dispersion relation analysis. The dispersion relation analysis calculates the diffusive and dispersive errors at each wavenumber, and by defining an appropriate tolerance, we can determine if a wave is resolved or not based on these errors.

The results show that the spatial order of accuracy appears to dominate a scheme's effective resolution, and that increasing the spatial order of accuracy of the numerical scheme increases the scheme's effective resolution regardless of the time-stepping scheme used. When increasing the spatial order of accuracy of a scheme by one, the greatest improvement is found for low order schemes (for example increasing from first- to second-order, or from second- to third-order), whereas the improvement diminishes for higher-order schemes. The results verify the conclusions of [15,40] that fourth-order accuracy appears to be 'optimal' in terms of improvement in accuracy relative to computational cost (note that [15] only considered spatial finite-differences). It can be shown that for some schemes increasing the order of accuracy is more beneficial, in terms of effective resolution, than just doubling the grid resolution. The sensitivity to the order of the time-stepping scheme is more complex and less predictable. While the Runge–Kutta schemes' effective resolution is largely independent of the Courant number, this is not the case for the other time-stepping schemes. The same results are found with the semi-Lagrangian and finite-volume schemes.

Explicit diffusion, hyper-diffusion, and the use of the Robert–Asselin filter increase the diffusion errors but can reduce the dispersion errors. This suggests that an optimal balance between diffusion and dispersion errors can increase the effective resolution of a scheme. This explicit diffusion is fundamentally an 'error' as this analysis is applied to the advection equation at constant velocity, for which there is formally no diffusion. For advection in sheared flows and in dynamical cores of weather and climate models diffusion is required to model the downscale cascade of certain quantities, and this physical diffusion also impacts the balance between diffusive and dispersive errors. These conflated roles of diffusion are a fundamental attribute of numerical advection schemes, and need to be considered not only in design but in analysis of the performance of the model.

The effective resolution of a numerical scheme is an important point to consider when developing a transport scheme for a dynamical core. For a GCM using $1^\circ \times 1^\circ$ resolution, the grid spacing at the equator is approximately 110 km. As shown for both finite-differences and finite-volumes, a second-order scheme may only fully resolve around $18 - 26\Delta x$ at low Courant numbers. This will correspond to the 1° GCM being unable to resolve fully features smaller than $\sim$2000–2800 km. For models with variable resolution grids, it is possible for the numerical scheme to lose an order-of-accuracy at the change in resolution [8]. Therefore a second-order scheme on a variable resolution grid might revert to first-order at the resolution

change, and, as shown in Fig. 1, could find the effective resolution drop by $20\Delta x$, possibly negating the benefits of the variable resolution mesh.

The analysis performed in this paper can be used to assess numerical advection schemes. It also provides robust guidance in optimizing the choice of spatial resolution, which influences the decisions about computational design and resource management. For example these measurements of effective resolution may indicate the comparative utility in increasing grid resolution as opposed to altering the algorithm itself to achieve a higher effective resolution. With regards to the effect of a chosen timestep, the analysis with this method reveals that the dependence of the effective resolution on the Courant number is significant. The analysis in this paper can only be applied to linear schemes, and does not inform us directly about non-linear schemes such as those with flux-limiters. However, this methodology has been modified to obtain similar measures of effective resolution for non-linear numerical schemes, and this will appear in a future paper. Although the advection scheme is far removed from a non-linear dynamical core, the inevitable gap between the grid-scale and effective resolution provides an important insight into the description of uncertainty that is associated with dynamical cores, such as variable resolution grids, land-water boundaries, steep topography and grid-scale physics.

Acknowledgements

We thank the reviewers for their helpful comments. This work was supported by the Office of Science, U.S. Department of Energy, Award No. DE-SC0006684.

References

[1] H. Aluie, S. Kurien, Joint downscale fluxes of energy and potential enstrophy in rotating stratified Boussinesq flows, Europhys. Lett. 96 (2011) 44006.
[2] R. Asselin, Frequency filter for time integrations, Mon. Weather Rev. 100 (1972) 487–490.
[3] P. Colella, P.R. Woodward, The piecewise parabolic method (PPM) for gas-dynamical simulations, J. Comput. Phys. 54 (1984) 174–201.
[4] T. Davies, M.J.P. Cullen, A.J. Malcom, M.H. Mawson, A. Staniforth, A.A. White, N. Wood, A new dynamical core for the Met Office's global and regional modelling of the atmosphere, Q. J. R. Meteorol. Soc. 131 (2005) 1759–1782.
[5] J.M. Dennis, J. Edwards, K.J. Evans, O. Guba, P.H. Lauritzen, A.A. Mirin, A. St-Cyr, M.A. Taylor, P.H. Worley, CAM-SE: a scalable spectral element dynamical core for the community atmosphere model, Int. J. High Perform. Comput. Appl. 26 (2012) 74–89.
[6] M. Dubal, A. Staniforth, N. Wood, Some numerical properties of approaches to physics-dynamics coupling for NWP, Q. J. R. Meteorol. Soc. 132 (2006) 27–42.
[7] D.R. Durran, The third-order Adams–Bashforth method: an attractive alternative to leapfrog time differencing, Mon. Weather Rev. 119 (1991) 702–720.
[8] M.S. Fox-Rabinovitz, G.L. Stenchikov, M.J. Suarez, L.L. Takacs, A finite-difference GCM dynamical core with a variable-resolution stretched grid, Mon. Weather Rev. 125 (1997) 2943–2968.
[9] S. Gottlieb, D.I. Ketcheson, C.-W. Shu, Strong Stability Preserving Runge–Kutta and Multistep Time Discretizations, World Scientific Publishing, New Jersey, USA, 2011.
[10] F.Q. Hu, M.Y. Hussaini, P. Rasetarinera, An analysis of the discontinuous Galerkin method for wave propagation problems, J. Comput. Phys. 151 (1999) 921–946.
[11] W.B. Hundsdorfer, B. Koren, M. van Loon, J.G. Verwer, A positive finite-difference advection scheme, J. Comput. Phys. 117 (1995) 35–46.
[12] C. Jablonowski, D.L. Williamson, The pros and cons of diffusion, filters and fixers in atmospheric general circulation models, in: P.H. Lauritzen, C. Jablonowski, M.A. Taylor, R.D. Nair (Eds.), Numerical Techniques for Global Atmospheric Models, Springer, 2011, pp. 381–493.
[13] J. Kent, J. Thuburn, N. Wood, Assessing implicit large eddy simulation for two-dimensional flow, Q. J. R. Meteorol. Soc. 138 (2012) 365–375.
[14] J. Kent, C. Jablonowski, J.P. Whitehead, R.B. Rood, Downscale cascades in tracer transport test cases: an intercomparison of the dynamical cores in the Community Atmosphere Model CAM5, Geosci. Model Dev. 5 (2012) 1517–1530.
[15] H.-O. Kreiss, J. Oliger, Comparison of accurate methods for the integration of hyperbolic equations, Tellus 24 (1972) 199–215.
[16] J. Lander, B. Hoskins, Believable scales and parameterizations in a spectral transform model, Mon. Weather Rev. 125 (1997) 292–303.
[17] P.H. Lauritzen, A stability analysis of finite-volume advection schemes permitting long time steps, Mon. Weather Rev. 135 (2009) 2658–2673.
[18] P.H. Lauritzen, R.D. Nair, P.A. Ullrich, A Conservative semi-Lagrangian multi-tracer transport scheme (CSLAM) on the cubed-sphere grid, J. Comput. Phys. 229 (2010) 1401–1424.
[19] P.D. Lax, B. Wendroff, Systems of conservation laws, Commun. Pure Appl. Math. 13 (1960) 217–237.
[20] S.J. Lin, A "vertically Lagrangian" finite-volume dynamical core for global models, Mon. Weather Rev. 132 (2004) 2293–2307.
[21] S.J. Lin, R.B. Rood, Multidimensional flux-form semi-Lagrangian transport schemes, Mon. Weather Rev. 124 (1996) 2046–2070.
[22] D. Long, J. Thuburn, Numerical wave propagation on non-uniform one-dimensional staggered grids, J. Comput. Phys. 230 (2011) 2643–2659.
[23] P.J. Mason, Large-eddy simulation: A critical review of the technique, Q. J. R. Meteorol. Soc. 120 (1994) 1–26.
[24] A. McDonald, Accuracy of multiply-upstream, semi-Lagrangian advective schemes, Mon. Weather Rev. 112 (1984) 1267–1275.
[25] T. Melvin, A. Staniforth, J. Thuburn, Dispersion analysis of the spectral element method, Q. J. R. Meteorol. Soc. 138 (2012) 1934–1947, http://dx.doi.org/10.1002/qj.1906.
[26] R.B. Neale, C.-C. Chen, A. Gettelman, P.H. Lauritzen, S. Park, D.L. Williamson, A.J. Conley, R. Garcia, D. Kinnison, J.-F. Lamarque, D. Marsh, M. Mills, A.K. Smith, S. Tilmes, F. Vitt, P. Cameron-Smith, W.D. Collins, M.J. Iacono, P.J. Rasch, M.A. Taylor, Description of the NCAR community atmosphere model (CAM 5.0), NCAR Tech. Note NCAR/TN-486+STR 2010, pp. 1–268.
[27] M.R. Norman, H. Finkel, Multi-moment ADER-Taylor methods for systems of conservation laws with source terms in one dimension, J. Comput. Phys. 231 (2012) 6622–6642.
[28] D. Randall, Geostrophic adjustment and the finite-difference shallow-water equations, Mon. Weather Rev. 122 (1994) 1371–1377.
[29] A. Robert, The integration of a low order spectral form of the primitive meteorological equations, J. Meteorol. Soc. Jpn. 44 (1966) 237–245.
[30] R.B. Rood, Numerical advection algorithms and their role in atmospheric transport and chemistry models, Rev. Geophys. 25 (1987) 71–100.
[31] W.C. Skamarock, Evaluating mesoscale NWP models using kinetic energy spectra, Mon. Weather Rev. 132 (2004) 3019–3032.
[32] W.C. Skamarock, A linear analysis of the NCAR CCSM finite-volume dynamical core, Mon. Weather Rev. 136 (2008) 2112–2119.
[33] J. Thuburn, Some conservation issues for the dynamical cores of NWP and climate models, J. Comput. Phys. 227 (2008) 3715–3730.
[34] E.F. Toro, R.C. Millington, L.A.M. Nejad, Towards very high order Godunov schemes, in: E.F. Toro (Ed.), Godunov Methods: Theory and Applications, Kluwer Academic/Plenum Publishers, New York, 2001, pp. 907–940.

[35] C.J. Tremback, J. Powell, W.R. Cotton, R.A. Pielke, The forward-in-time upstream advection scheme: extension to higher orders, Mon. Weather Rev. 115 (1987) 540–555.
[36] P.A. Ullrich, C. Jablonowski, An analysis of 1D finite-volume methods for geophysical problems on refined grids, J. Comput. Phys. 230 (2011) 706–725.
[37] P.A. Ullrich, C. Jablonowski, Operator-split Runge–Kutta–Rosenbrock (RKR) methods for nonhydrostatic atmospheric models, Mon. Weather Rev. 140 (2011) 1257–1284.
[38] P.A. Ullrich, C. Jablonowski, MCore: A nonhydrostatic atmospheric dynamical core utilizing high-order finite-volume methods, J. Comput. Phys. 231 (2012) 5078–5108.
[39] P.A. Ullrich, M.R. Norman, The flux-form semi-Lagrangian spectral element (FF-SLSE) method for tracer transport, Q. J. R. Meteorol. Soc. (2014), http://dx.doi.org/10.1002/qj.2184.
[40] P.A. Ullrich, Understanding the treatment of waves in atmospheric models. Part 1: The shortest resolved waves of the 1D linearized shallow-water equations, Q. J. R. Meteorol. Soc. (2014), http://dx.doi.org/10.1002/qj.2226.
[41] M.K. Walters, Comments on "The differentiation between grid spacing and resolution and their application to numerical modeling", Bull. Am. Meteorol. Soc. 81 (2000) 2475–2477.
[42] J.P. Whitehead, C. Jablonowski, R.B. Rood, P.H. Lauritzen, A stability analysis of divergence damping on a latitude–longitude grid, Mon. Weather Rev. 139 (2011) 2976–2993.
[43] L.J. Wicker, W.C. Skamarock, Time-splitting methods for elastic models using forward time schemes, Mon. Weather Rev. 130 (2002) 2088–2097.
[44] D.L. Williamson, Convergence of atmospheric simulations with increasing horizontal resolution and fixed forcing scales, Tellus A 51 (1999) 663–673.
[45] D.L. Williamson, The evolution of dynamical cores for global atmospheric models, J. Meteorol. Soc. Jpn. B 85 (2007) 241–269.
[46] D.L. Williamson, Equivalent finite volume and Eulerian spectral transform horizontal resolutions established from aqua-planet simulations, Tellus A 60 (2008) 839–847.
[47] D.L. Williamson, J.G. Olson, Climate simulations with a semi-Lagrangian version of the NCAR Community Climate Model, Mon. Weather Rev. 122 (1994) 1594–1610.
[48] M. Zerroukat, N. Wood, A. Staniforth, SLICE: a semi-Lagrangian inherently conserving and efficient scheme for transport problems, Q. J. R. Meteorol. Soc. 128 (2002) 2801–2820.